

SYNTHESIS, CHARACTERIZATION AND *IN VITRO* EVALUATION OF CYTOTOXIC POTENTIAL OF MONO, DI, TRI AND TETRA N-HETEROCYCLIC CARBENE SILVER(I) COMPLEXES

TABINDA FATIMA

UNIVERSITI SAINS MALAYSIA

2017

SYNTHESIS, CHARACTERIZATION AND *IN VITRO* EVALUATION OF CYTOTOXIC POTENTIAL OF MONO, DI, TRI AND TETRA *N*-HETEROCYCLIC CARBENE SILVER(I) COMPLEXES

by

TABINDA FATIMA

**Thesis submitted in fulfilment of the requirements
for the degree of
Doctor of Philosophy**

May 2017

Dedication

I dedicate this thesis to my loving husband, my parents and my sisters and brothers,
their love and support enabled me to complete my PhD.

ACKNOWLEDGEMENT

First of all I would like to pay extensive thanks to Almighty ALLAH, for giving me an opportunity and strength to complete a doctoral research in one of the world's prestigious universities, Universiti Sains Malaysia.

I would like to pay my gratitude to my supervisor, Associate Prof. Dr Rosenani A. Haque for being such a great supervisor and a great human being. Her continuous encouragement during the challenging period of my research, her advice, guidance, availability of her experience and knowledge in this field have always been there for a smooth progression of the work. I am also thankful to her for her moral support and counselling at a personal level. She is indeed a source of inspiration for me and will always stay high in my heart as long as I live.

I greatly acknowledge the contribution of my co-supervisor Dr Mohd. Rizal Razali for his guidance and insightful, friendly discussions, throughout the research work and the writing process. Thank you Dr Rizal for being such a helpful co-supervisor.

I wish to thank the Dean of the School of Chemical Sciences for providing the necessary research facilities and also to the academic, non-academic, technical and the supporting staff for always been facilitating.

I would also like to thank the Dean of IPS and the staff who had helped me in one way or another. I would like to acknowledge IPS for providing me the USM Fellowship award (APEX (1002/JHEA/ATSG4001).

I thank my group fellows Dr Muhammad Adnan Iqbal, Dr Patrick O. Asekunowo, Choo Sii Zye, Noor Hafizah, Umie Fatiah, Sunusi Yahya and Yeap Choon Wan for their friendship and support, we all had a great time together. I am

also very grateful to Nosheen Karamat for her moral support and to Zafar Iqbal and Arifa Zafar for their nice company during my stay in Malaysia. I would specially like to thank all the Hadhanah staff for taking good care of my daughter, thus enabling me to focus on my work.

I would like to express my very special thanks and love to my parents, sisters and brothers for their immense love and support. Last but not the least, my sincere thanks go to my beloved husband Ashfaq Ahmad and my daughter Zainab Fatima for their patience and sacrifices during my research time. The work would not be possible without their remarkable support and understanding.

TABLE OF CONTENTS

| | |
|--|----------|
| Acknowledgement | ii |
| Table of contents | iv |
| List of Tables | xii |
| List of Figures | xiv |
| List of Schemes | xxiii |
| List of Abbreviations | xxv |
| Abstrak | xxvii |
| Abstract | xxix |
| CHAPTER 1-INTRODUCTION | 1 |
| 1.1 The Carbenes | 1 |
| 1.2 Classification of carbenes | 3 |
| 1.2.1 Fischer carbenes | 3 |
| 1.2.2 Schrock carbenes | 4 |
| 1.2.3 <i>N</i> -heterocyclic carbenes | 5 |
| 1.3 Emergence of <i>N</i> -heterocyclic carbenes | 6 |
| 1.3.1 <i>N</i> -heterocyclic carbene complexes | 10 |
| 1.3.1(a) <i>In situ</i> deprotonation of azolium salts | 11 |
| 1.3.1(b) Free carbene route | 12 |
| 1.3.1(c) Ligand transfer reactions | 13 |
| 1.3.1(d) Cleavage of enetetraamines | 14 |
| 1.4 <i>N</i> -heterocyclic carbene silver(I) complexes | 15 |
| 1.4.1 Synthesis of <i>N</i> -heterocyclic carbenes silver(I) complexes | 15 |

| | | |
|----------|--|----|
| 1.4.1(a) | The free carbene method | 15 |
| 1.4.1(b) | The <i>in situ</i> deprotonation method | 16 |
| 1.4.2 | Classification of <i>N</i> -heterocyclic carbene silver(I) complexes | 18 |
| 1.4.2(a) | Mono NHC-Ag(I) complexes | 18 |
| 1.4.2(b) | Di NHC-Ag(I) complexes | 19 |
| 1.4.2(c) | Tri NHC-Ag(I) complexes | 20 |
| 1.4.2(d) | Tetra NHC-Ag(I) complexes | 21 |
| 1.5 | Applications of <i>N</i> -heterocyclic carbene silver(I) complexes | 22 |
| 1.5.1 | Carbene transfer agents in transmetallation | 22 |
| 1.5.2 | Catalysts | 26 |
| 1.5.3 | Biological activity of silver compounds | 27 |
| 1.5.3(a) | Medicinal importance of silver | 27 |
| 1.5.3(b) | Cancer and anticancer agents | 29 |
| 1.5.3(c) | NHC-Ag(I) complexes – suitable candidates for Ag(I) metallodrugs | 30 |
| 1.5.3(d) | NHC-Ag(I) complexes as potential antitumor metallodrugs | 31 |
| 1.5.3(e) | Mechanism of cancer cell death caused by NHC-Ag(I) complexes | 34 |
| 1.6 | Problem statement | 35 |
| 1.7 | Objectives of the present research | 36 |
| | CHAPTER 2-EXPERIMENTAL | 38 |
| 2.1 | Materials | 38 |
| 2.2 | Characterization Techniques | 39 |
| 2.2.1 | Melting point determination | 39 |

| | | |
|-------|---|----|
| 2.2.2 | CHN Elemental microanalysis | 39 |
| 2.2.3 | Infra Red Spectroscopy | 39 |
| 2.2.4 | Nuclear Magnetic Resonance Spectroscopy | 39 |
| 2.2.5 | X-Ray Diffraction | 40 |
| 2.3 | Synthesis of mono benzimidazolium bromides (1-8) | 40 |
| 2.3.1 | <i>N,N-n</i> -propylbenzimidazolium bromide (1) | 41 |
| 2.3.2 | <i>N,N-n</i> -butylbenzimidazolium bromide (2) | 41 |
| 2.3.3 | <i>N,N-n</i> -pentylbenzimidazolium bromide (3) | 42 |
| 2.3.4 | <i>N,N-n</i> -hexylbenzimidazolium bromide (4) | 43 |
| 2.3.5 | <i>N,N-n</i> -heptylbenzimidazolium bromide (5) | 44 |
| 2.3.6 | <i>N,N-n</i> -octylbenzimidazolium bromide (6) | 44 |
| 2.3.7 | <i>N,N-n</i> -nonylbenzimidazolium bromide (7) | 45 |
| 2.3.8 | <i>N,N-n</i> -decylbenzimidazolium bromide (8) | 46 |
| 2.4 | Synthesis of bis benzimidazolium bromides (9-16) | 47 |
| 2.4.1 | Tetramethylenebis(<i>N-n</i> -propylbenzimidazolium bromide) (9) | 47 |
| 2.4.2 | Tetramethylenebis(<i>N-n</i> -butylbenzimidazolium bromide) (10) | 48 |
| 2.4.3 | Tetramethylenebis(<i>N-n</i> -pentylbenzimidazolium bromide) (11) | 48 |
| 2.4.4 | Tetramethylenebis(<i>N-n</i> -hexylbenzimidazolium bromide) (12) | 49 |
| 2.4.5 | Tetramethylenebis(<i>N-n</i> -heptylbenzimidazolium bromide) (13) | 50 |
| 2.4.6 | Tetramethylenebis(<i>N-n</i> -octylbenzimidazolium bromide) (14) | 51 |
| 2.4.7 | Tetramethylenebis(<i>N-n</i> -nonylbenzimidazolium bromide) (15) | 51 |

| | | |
|-------|---|----|
| 2.4.8 | Tetramethylenebis(<i>N-n</i> -decylbenzimidazolium bromide)(16) | 52 |
| 2.5 | Synthesis of 3-(2-bromoethyl)-1-substituted benzimidazolium bromides (17-21) | 53 |
| 2.5.1 | 3-(2-bromoethyl)-1-benzyl benzimidazolium bromide (17) | 54 |
| 2.5.2 | 3-(2-bromoethyl)-1- <i>n</i> -butyl benzimidazolium bromide (18) | 55 |
| 2.5.3 | 3-(2-bromoethyl)-1-cyclopentylbenzimidazolium bromide (19) | 56 |
| 2.5.4 | 3-(2-bromoethyl)-1-(2-methylene benzonitrile) benzimidazolium bromide (20) | 57 |
| 2.5.5 | 3-(2-chloroethyl)-1- <i>n</i> -decyl benzimidazolium bromide (21) | 57 |
| 2.6 | Synthesis of tris benzimidazolium bromides (22-26) | 58 |
| 2.6.1 | benzyl substituted tris benzimidazolium bromide (22) | 58 |
| 2.6.2 | <i>n</i> -butyl substituted tris benzimidazolium bromide (23) | 59 |
| 2.6.3 | cyclopentyl substituted tris benzimidazolium bromide (24) | 60 |
| 2.6.4 | 2-methylenebenzonitrile substituted tris benzimidazolium bromide (25) | 61 |
| 2.6.5 | <i>n</i> -decyl substituted tris benzimidazolium bromide (26) | 61 |
| 2.7 | Synthesis of tetrakis benzimidazolium bromides (27-31) | 62 |
| 2.7.1 | Synthesis of 1,2-bis(benzimidazol-1-ylmethyl)benzene | 62 |
| 2.7.2 | benzyl substituted tetrakis benzimidazolium bromide (27) | 63 |
| 2.7.3 | <i>n</i> -butyl substituted tetrakis benzimidazolium bromide (28) | 64 |
| 2.7.4 | cyclopentyl substituted tetrakis benzimidazolium bromide (29) | 65 |
| 2.7.5 | 2- methylenebenzonitrile substituted tetrakis benzimidazolium bromide (30) | 66 |
| 2.7.6 | <i>n</i> -decyl substituted tetrakis benzimidazolium bromide (31) | 66 |

| | | |
|-------|--|----|
| 2.8 | Synthesis of mono NHC-Ag(I) complexes (32-39) | 67 |
| 2.8.1 | <i>N,N-n</i> -propylbenzimidazol-2-ylidenesilver(I) hexafluorophosphate (32) | 67 |
| 2.8.2 | <i>N,N-n</i> -butylbenzimidazol-2-ylidenesilver(I) hexafluorophosphate (33) | 68 |
| 2.8.3 | <i>N,N-n</i> -pentylbenzimidazol-2-ylidenesilver(I) hexafluorophosphate (34) | 69 |
| 2.8.4 | <i>N,N-n</i> -hexylbenzimidazol-2-ylidenesilver(I) hexafluorophosphate (35) | 70 |
| 2.8.5 | <i>N,N-n</i> -heptylbenzimidazol-2-ylidenesilver(I) hexafluorophosphate (36) | 71 |
| 2.8.6 | <i>N,N-n</i> -octylbenzimidazol-2-ylidenesilver(I) hexafluorophosphate (37) | 72 |
| 2.8.7 | <i>N,N-n</i> -nonylbenzimidazol-2-ylidenesilver(I) hexafluorophosphate (38) | 73 |
| 2.8.8 | <i>N,N-n</i> -decylbenzimidazol-2-ylidene silver(I) hexafluorophosphate (39) | 74 |
| 2.9 | Synthesis of di NHC-Ag(I) complexes (40-47) | 75 |
| 2.9.1 | Tetramethylenebis{(<i>N-n</i> -propylbenzimidazol-2-ylidene)silver(I)hexafluorophosphate} (40) | 75 |
| 2.9.2 | Tetramethylenebis{(<i>N-n</i> -butylbenzimidazol-2-ylidene)silver hexafluorophosphate} (41) | 76 |
| 2.9.3 | Tetramethylenebis{(<i>N-n</i> -pentylbenzimidazol-2-ylidene)silver(I)hexafluorophosphate} (42) | 77 |
| 2.9.4 | Tetramethylenebis{(<i>N-n</i> -hexylbenzimidazol-2-ylidene)silver(I)hexafluorophosphate} (43) | 78 |
| 2.9.5 | Tetramethylenebis{(<i>N-n</i> -heptylbenzimidazol-2-ylidene)silver(I)hexafluorophosphate} (44) | 79 |
| 2.9.6 | Tetramethylenebis{(<i>N-n</i> -octylbenzimidazol-2-ylidene)silver(I)hexafluorophosphate} (45) | 80 |
| 2.9.7 | Tetramethylenebis{(<i>N-n</i> -nonylbenzimidazol-2-ylidene)silver(I)hexafluorophosphate} (46) | 81 |

| | | |
|-----------|--|-----|
| 2.9.8 | Tetramethylenebis{(N-n-decylbenzimidazol-2-ylidene)silver(I)hexafluorophosphate} (47) | 82 |
| 2.10 | Synthesis of tri NHC-Ag(I) complexes (48-52) | 83 |
| 2.10.1 | benzyl substituted tri NHC-Ag(I) complex (48) | 83 |
| 2.10.2 | n-butyl substituted tri NHC-Ag(I) complex (49) | 84 |
| 2.10.3 | cyclopentyl substituted tri NHC-Ag(I) complex (50) | 85 |
| 2.10.4 | 2-methylenebenzotrile substituted tri NHC-Ag(I) complex (51) | 86 |
| 2.10.5 | n-decyl substituted tri NHC-Ag(I) complex (52) | 87 |
| 2.11 | Synthesis of tetra NHC-Ag(I) complexes (53-57) | 88 |
| 2.11.1 | benzyl substituted tetra NHC-Ag(I) complex (53) | 88 |
| 2.11.2 | n-butyl substituted tetra NHC-Ag(I) complex (54) | 89 |
| 2.11.3 | cyclopentyl substituted tetra NHC-Ag(I) complex (55) | 90 |
| 2.11.4 | 2- methylenebenzotrile substituted tetra NHC-Ag(I) complex (56) | 91 |
| 2.11.5 | n-decyl substituted tetra NHC-Ag(I) complex (57) | 92 |
| 2.12 | <i>In vitro</i> cytotoxic studies | 93 |
| 2.12.1 | Materials and equipments | 93 |
| 2.12.2 | Cell lines and environmental conditions | 93 |
| 2.12.3 | Preparation of cell culture | 94 |
| 2.12.4 | MTT assay | 94 |
| 2.12.5 | Construction of standard curves of 5-FU and tamoxifen | 95 |
| 2.12.6 | Study of mode of cytotoxicity for tetra NHC dinuclear Ag(I) compounds | 99 |
| 2.12.6(a) | Cell migration assay of MCF-7 cells treated | 100 |

| | | |
|---|---|------------|
| | with selected proligand and respective tetra NHC dinuclear Ag(I) complex | |
| 2.12.6(b) | Colony formation assay on MCF-7 cell line treated with selected proligand and respective tetra NHC Ag(I) complex | 101 |
| 2.12.7 | Statistical analysis | 102 |
| CHAPTER 3-RESULTS AND DISCUSSION | | 103 |
| 3.1 | Preparation | 104 |
| 3.2 | Characterization | 114 |
| 3.2.1 | FTIR Analysis | 114 |
| 3.2.2 | ¹ H & ¹³ C-NMR Analysis | 117 |
| 3.2.3 | X-ray Crystallographic Analysis | 132 |
| CHAPTER 4-CYTOTOXICITY STUDIES | | 155 |
| 4.1 | <i>In vitro</i> cytotoxicity studies | 155 |
| 4.2 | <i>In vitro</i> cytotoxicity activities of mono NHC mononuclear Ag(I) complexes and the respective proligands against human colon cancer (HCT-116) cell lines | 158 |
| 4.3 | <i>In vitro</i> cytotoxicity activities of di NHC dinuclear Ag(I) complexes and their respective proligands against the human colon cancer (HCT116) cell lines | 169 |
| 4.4 | <i>In vitro</i> cytotoxicity activities of tri NHC trinuclear Ag(I) complexes and their respective proligands | 181 |
| 4.4.1 | <i>In vitro</i> cytotoxicity activities of tri NHC trinuclear Ag(I) complexes and their respective proligands against the human colon cancer (HCT-116) cell lines | 181 |
| 4.4.2 | <i>In vitro</i> cytotoxicity activities of tri NHC trinuclear Ag(I) complexes and their respective proligands against the breast cancer (MCF-7) cell lines | 186 |

| | | |
|----------|--|-----|
| 4.4.3 | <i>In vitro</i> cytotoxicity activities of tri NHC trinuclear Ag(I) complexes and their respective proligands against the human epitheloid cervix carcinoma (HeLa) cell lines | 190 |
| 4.5 | <i>In vitro</i> cytotoxicity activities of tetra NHC dinuclear Ag(I) complexes and their respective proligands | 195 |
| 4.5.1 | <i>In vitro</i> cytotoxicity activities of tetra NHC dinuclear Ag(I) complexes and their respective proligands against the human colon cancer (HCT116) cell lines | 195 |
| 4.5.2 | <i>In vitro</i> cytotoxicity activities of tetra NHC dinuclear Ag(I) complexes and their respective proligands against the breast cancer (MCF-7) cell lines | 197 |
| 4.5.3 | <i>In vitro</i> cytotoxicity activities of the tetra NHC dinuclear Ag(I) complexes and their respective proligands against the human epitheloid cervix carcinoma (HeLa) cell lines | 201 |
| 4.5.4 | Study of mode of the cytotoxic activity of the selected tetra NHC dinuclear Ag(I) complex 57 and their respective proligand 31 | 206 |
| 4.5.4(a) | Cell migration assay for the proligand 31 and the complex 57 | 206 |
| 4.5.4(b) | Colony formation assay for the proligand 31 and the complex 57 | 211 |
| 4.6 | Comparison of cytotoxic activities between mono, di, tri and tetra NHC-Ag(I) complexes and the respective proligands containing longest carbon chain length (C-10) | 215 |

CHAPTER 5-CONCLUSIONS AND RECOMMENDATIONS FOR

| | |
|---|-----|
| FUTURE WORK | 221 |
| 5.1 Conclusions | 221 |
| 5.2 Recommendations for future work | 223 |
| REFERENCES | 226 |
| LIST OF PUBLICATIONS AND CONFERENCES | 247 |

LIST OF TABLES

| | | Page |
|-----------|--|-------------|
| Table 2.1 | Spectrophotometric absorbance of known concentrations of 5-FU and Tamoxifen (0.78-25 μg) for construction of calibration curve. | 96 |
| Table 3.1 | Selected bond lengths [\AA] and angles [$^\circ$] for salts 3 and 7 . | 133 |
| Table 3.2 | Selected bond lengths [\AA] and angles [$^\circ$] for complexes 38 and 39 . | 136 |
| Table 3.3 | Selected bond lengths [\AA] and angles [$^\circ$] for complexes 45 and 47 . | 141 |
| Table 3.4 | Selected bond lengths [\AA] and angles [$^\circ$] for salts 17 and 19 . | 144 |
| Table 3.5 | Selected bond lengths [\AA] and angles [$^\circ$] for salts 18 and 21 . | 146 |
| Table 3.6 | Selected bond lengths [\AA] and angles [$^\circ$] for salt 22 . | 148 |
| Table 3.7 | Selected bond lengths [\AA] and angles [$^\circ$] for complexes 55 . | 152 |
| Table 4.1 | IC_{50} values of the proligands/salts (1-8) and their respective NHC-Ag(I) complexes (32-39) on HCT 116 using the standard 5-FU ($\text{IC}_{50} = 10.2 \mu\text{M}$). | 159 |
| Table 4.2 | IC_{50} values of the proligands/salts (9-16) and their respective NHC-Ag(I) complexes (40-47) on HCT 116 using the standard drug 5-FU ($\text{IC}_{50} = 10.2 \mu\text{M}$) as positive control. | 172 |
| Table 4.3 | IC_{50} values of the proligands (22-26) and their respective complexes (48-52) on HCT 116 and EA.hy926 using the standard drug 5-FU ($\text{IC}_{50} = 10.2 \mu\text{M}$) as positive control. | 183 |
| Table 4.4 | IC_{50} values of proligands (22-26) and complexes (48-52) on MCF-7 using the standard drug Tamoxifen ($\text{IC}_{50} = 7.5 \mu\text{M}$) as positive control. | 186 |
| Table 4.5 | IC_{50} values of proligands (22-26) and complexes (48-52) on the HeLa cell lines using the standard drug 5-FU ($\text{IC}_{50} = 10.2 \mu\text{M}$) as positive control. | 190 |
| Table 4.6 | IC_{50} values of proligand- 31 , and the complexes- 53 and 57 on HCT 116 using the standard drug 5-FU ($\text{IC}_{50} = 10.2 \mu\text{M}$) as positive control. | 195 |

| | | |
|-----------|---|-----|
| Table 4.7 | IC ₅₀ values of proligand- 31 and complexes (53-57) on the MCF-7 cell lines and the EA.hy926 cell lines using the standard Tamoxifen drug (IC ₅₀ = 7.5μM) as positive control. | 198 |
| Table 4.8 | IC ₅₀ values of proligand- 31 and complexes (53-57) on the HeLa cell lines using the standard drug 5-FU (IC ₅₀ = 10.2 μM) as positive control. | 202 |
| Table 4.9 | IC ₅₀ values of proligands (8, 16, 26, 31) and complexes (39, 47, 52, 57) on the human colon cancer cell line (HCT 116) using the standard drug 5-FU (IC ₅₀ = 10.2 μM) as positive control. | 216 |

LIST OF FIGURES

| | | Page |
|-------------|--|-------------|
| Figure 1.1 | Representation of spin multiplicities of sp^2 hybridized carbenes. | 2 |
| Figure 1.2 | Carbene to metal bonding in Fischer carbene. | 4 |
| Figure 1.3 | Carbene to metal bonding in Schrock carbene. | 5 |
| Figure 1.4 | Carbene to metal bonding in <i>N</i> -heterocyclic carbene. | 5 |
| Figure 1.5 | Structures of reported stable carbenes (a-f) by Arduengo. | 9 |
| Figure 1.6 | Structures of some most commonly applied classes of NHCs. | 10 |
| Figure 1.7 | Structural variations of mono NHC-Ag(I) complexes. | 19 |
| Figure 1.8 | Structural variations of di NHC-Ag(I) complexes. | 20 |
| Figure 1.9 | Structural variations of tri NHC-Ag(I) complexes. | 21 |
| Figure 1.10 | Some structural variations of tetra NHC-Ag(I) complexes. | 22 |
| Figure 1.11 | Structures of some anticancer drugs (a) cisplatin (b) 5-fluorouracil. | 30 |
| Figure 1.12 | Some NHC-Ag(I) complexes having anticancer activity comparable to cisplatin reported by (a) Youngs et al. (b) Gautier et al. (c) Tacke et al. (d) Willans et al. | 33 |
| Figure 2.1 | 96 wells microplate used in MTT assay. | 97 |
| Figure 2.2 | Calibration curve for 5-FU. | 97 |
| Figure 2.3 | Calibration curve for Tamoxifen. | 98 |
| Figure 3.1 | Representative FTIR spectra of salt 7 (top) and respective mono NHC-Ag(I) complex 38 (bottom). | 115 |
| Figure 3.2 | Representative FTIR spectra of salt 14 (top) and respective di NHC-Ag(I) complex 45 (bottom). | 116 |
| Figure 3.3 | Representative FTIR spectra of salt 25 (top) and respective tri NHC-Ag(I) complex 51 (bottom). | 116 |

| | | |
|-------------|---|-----|
| Figure 3.4 | Representative FTIR spectra of salt 30 (top) and respective tetra NHC-Ag(I) complex 56 (bottom). | 117 |
| Figure 3.5 | ¹ H NMR spectrum (<i>d</i> ₆ -DMSO, 500 MHz) of salt 2 , indicating the chemical shifts of all types of protons highlighting the resonance of the C2-proton(H <i>e</i>) which is an indication of a successful synthesis of mono benzimidazolium salt. | 118 |
| Figure 3.6 | ¹³ C NMR spectrum (<i>d</i> ₆ -DMSO, 125 MHz) of salt 2 , highlighting the resonance of most deshielded C-2 carbon (precarbenic carbon). | 119 |
| Figure 3.7 | ¹ H NMR spectrum (<i>d</i> ₆ -DMSO, 500 MHz) of salt 16 , indicating the chemical shifts of all types of protons highlighting the resonance of the C2-protons (H <i>g</i>) which is an indication of a successful synthesis of bis benzimidazolium salt. | 120 |
| Figure 3.8 | ¹³ C NMR spectrum (<i>d</i> ₆ -DMSO, 125 MHz) of salt 16 , highlighting the resonance of most deshielded C-2 carbon (precarbenic carbon). | 121 |
| Figure 3.9 | ¹ H NMR spectrum (<i>d</i> ₆ -DMSO, 500 MHz) of salt 22 , indicating the chemical shifts of all types of protons, highlighting the resonance signals for two types of acidic protons (H <i>c</i> and H <i>d</i>) which is an indication of a successful synthesis of tris benzimidazolium salt. | 122 |
| Figure 3.10 | ¹³ C NMR spectrum (<i>d</i> ₆ -DMSO, 125 MHz) of salt 22 , highlighting the resonances of most deshielded C-2 carbons (precarbenic carbons). | 123 |
| Figure 3.11 | ¹ H NMR spectrum (<i>d</i> ₆ -DMSO, 500 MHz) of salt 29 , indicating the chemical shifts of all types of protons highlighting the resonance of two types of the C2-acidic protons (H <i>f</i> and H <i>g</i>) which is an indication of a successful synthesis of tetrakis benzimidazolium salt. | 125 |
| Figure 3.12 | ¹³ C NMR spectrum (<i>d</i> ₆ -DMSO, 125 MHz) of salt 29 , highlighting the resonances of most deshielded C-2 carbons (precarbenic carbons). | 125 |
| Figure 3.13 | ¹³ H NMR spectrum (<i>d</i> ₃ -acetonitrile, 500 MHz) of mono NHC-Ag(I) complex 33 , highlighting the disappearance of the resonance of the acidic proton (NCHN), which is an indication of a successful complexation. | 127 |

| | | |
|-------------|--|-----|
| Figure 3.14 | ^{13}C NMR spectrum (d_3 -acetonitrile, 125 MHz) of mono NHC-Ag(I) complex 33 , highlighting the appearance of the resonances for the carbene-Ag bond which is an indication of a successful complexation. | 127 |
| Figure 3.15 | ^1H NMR spectrum (d_3 -acetonitrile, 500 MHz) of di NHC-Ag(I) complex 47 , highlighting the disappearance of resonances of the acidic protons (NCHN) of the proligand, which is an indication of a successful complexation. | 129 |
| Figure 3.16 | ^{13}C NMR spectrum (d_3 -acetonitrile, 125 MHz) of di NHC-Ag(I) complex 47 , highlighting the appearance of the resonances of the carbene-Ag bond which is an indication of a successful complexation. | 129 |
| Figure 3.17 | ^{13}C NMR spectrum (d_3 -acetonitrile, 125 MHz) of tri NHC-Ag(I) complex 48 , highlighting the appearance of the resonance signal for the two types of carbene-Ag bonds which is an indication of a successful synthesis of the tri NHC-Ag(I) complex. | 130 |
| Figure 3.18 | ^{13}C NMR spectrum (d_3 -acetonitrile, 125 MHz) of tetra NHC-Ag(I) complex 55 , highlighting the appearance of the resonances of the carbene-Ag bond which is an indication of a successful complexation. | 132 |
| Figure 3.19 | ORTEP diagram of salt 3 , showing 50% probability ellipsoids. | 134 |
| Figure 3.20 | ORTEP diagram of salt 7 , showing 50% probability ellipsoids. | 134 |
| Figure 3.21 | Crystal packing of salt 7 showing the hydrogen bonds as dashed lines. | 135 |
| Figure 3.22 | ORTEP diagram of complex 38 , showing 50% probability ellipsoids. | 137 |
| Figure 3.23 | Crystal packing of complex 38 . | 138 |
| Figure 3.24 | ORTEP diagram of complex 39 , showing 50% probability ellipsoids. | 139 |
| Figure 3.25 | ORTEP diagram of complex 45 , showing 50% probability ellipsoids. | 141 |
| Figure 3.26 | Crystal packing of complex 45 . | 142 |
| Figure 3.27 | ORTEP diagram of complex 47 , showing 50% probability. | 142 |

| | | |
|-------------|---|-----|
| Figure 3.28 | Crystal packing of complex 47 . | 143 |
| Figure 3.29 | ORTEP diagram of salt 17 , showing 50% probability ellipsoids. | 145 |
| Figure 3.30 | ORTEP diagram of salt 19 , showing 50% probability ellipsoids. | 145 |
| Figure 3.31 | ORTEP diagram of salt 18 , showing 50% probability ellipsoids. | 147 |
| Figure 3.32 | ORTEP diagram of salt 21 , showing 50% probability ellipsoids. | 147 |
| Figure 3.33 | ORTEP diagram of salt 22 , showing 50% probability ellipsoids. | 149 |
| Figure 3.34 | Crystal packing of salt 22 . | 150 |
| Figure 3.35 | (a) ORTEP diagram of complex 55 , showing 50% probability ellipsoids. (b) Hydrogen atoms are omitted for the purpose of clarity. | 153 |
| Figure 3.36 | Crystal packing of complex 55 . | 154 |
| Figure 4.1 | Anatomical position of colon in the gastrointestinal tract (adapted from http://www.webmd.com/digestive-disorders). | 155 |
| Figure 4.2 | Dose dependent proliferative effects of proligand 1 and complex 32 in comparison with the standard drug 5-FU. | 160 |
| Figure 4.3 | Dose dependent proliferative effects of proligand 2 and complex 33 in comparison with the standard drug 5-FU. | 161 |
| Figure 4.4 | Dose dependent proliferative effects of proligand 3 and complex 34 in comparison with the standard drug 5-FU. | 161 |
| Figure 4.5 | Dose dependent proliferative effects of proligand 4 and complex 35 in comparison with the standard drug 5-FU. | 163 |
| Figure 4.6 | Dose dependent proliferative effects of proligand 5 and complex 36 in comparison with the standard drug 5-FU. | 163 |
| Figure 4.7 | Dose dependent proliferative effects of proligand 6 and complex 37 in comparison with the standard drug 5-FU. | 164 |
| Figure 4.8 | Dose dependent proliferative effects of proligand 7 and complex 38 in comparison with the standard drug 5-FU. | 164 |

| | | |
|---------------|--|-----|
| Figure 4.9 | Dose dependent proliferative effects of proligand 8 and complex 39 in comparison with the standard drug 5-FU. | 165 |
| Figure 4.10-A | Human colorectal tumor (HCT-116) cell images captured under a light microscope at × 200 magnification with a digital camera at 48 hours after the treatment with proligands 1-3 and their respective complexes 32-34 . | 166 |
| Figure 4.10-B | Human colorectal tumor (HCT 116) cell images taken under a light microscope at × 200 magnification with a digital camera at 48 hours after the treatment with proligands 4-8 and their respective complexes 35-39 . | 168 |
| Figure 4.11 | Dose dependent proliferative effects of proligand 9 and complex 40 in comparison with the standard drug 5-FU. | 173 |
| Figure 4.12 | Dose dependent proliferative effects of proligand 10 and complex 41 in comparison with the standard drug 5-FU. | 173 |
| Figure 4.13 | Dose dependent proliferative effects of proligand 11 and complex 42 in comparison with the standard drug 5-FU. | 174 |
| Figure 4.14 | Dose dependent proliferative effects of proligand 12 and complex 43 in comparison with the standard drug 5-FU. | 174 |
| Figure 4.15 | Dose dependent proliferative effects of proligand 13 and complex 44 in comparison with the standard drug 5-FU. | 175 |
| Figure 4.16 | Dose dependent proliferative effects of proligand 14 and complex 45 in comparison with the standard drug 5-FU. | 175 |
| Figure 4.17 | Dose dependent proliferative effects of proligand 15 and complex 46 in comparison with the standard drug 5-FU. | 176 |
| Figure 4.18 | Dose dependent proliferative effects of proligand 16 and complex 47 in comparison with the standard drug 5-FU. | 176 |
| Figure 4.19-A | Human colorectal tumor (HCT 116) cell images taken under a light microscope at × 200 magnification with a digital camera at 48 hours after treatment with the proligands (9-11) and their respective complexes (40-42). | 179 |
| Figure 4.19-B | Human colorectal tumor (HCT 116) cell images taken under a light microscope at × 200 magnification with a digital camera at 48 hours after treatment with the proligands (12-16) and their respective complexes (43-47). | 180 |
| Figure 4.20 | Dose dependent proliferative effects of complex 51 against the human colon cancer cell lines in comparison with the standard drug 5-FU. | 184 |

| | | |
|-------------|--|-----|
| Figure 4.21 | Dose dependent proliferative effects of proligand 26 and complex 52 against the human colon cancer cell lines in comparison with standard drug 5-FU. | 184 |
| Figure 4.22 | Images of human colorectal cancer cell lines and human endothelial cell lines showing the effects of proligands 26 and complexes 51 & 52 . (cell images were taken under a light microscope at $\times 200$ magnification with a digital camera at 48 hours after treatment). | 185 |
| Figure 4.23 | Dose dependent antiproliferative effects of complex 49 against the breast cancer cell lines in comparison with the standard drug Tamoxifen. | 188 |
| Figure 4.24 | Dose dependent antiproliferative effects of complex 50 against the breast cancer cell lines in comparison with the standard drug Tamoxifen. | 188 |
| Figure 4.25 | Dose dependent antiproliferative effects of complex 51 against the breast cancer cell lines in comparison with the standard drug Tamoxifen. | 189 |
| Figure 4.26 | Dose dependent antiproliferative effects of proligand 26 and complex 52 against the breast cancer cell lines in comparison with the standard drug Tamoxifen. | 189 |
| Figure 4.27 | Dose dependent antiproliferative effects of complex 48 in comparison with the standard drug 5-FU. | 192 |
| Figure 4.28 | Dose dependent antiproliferative effects of complex 49 in comparison with the standard drug 5-FU. | 192 |
| Figure 4.29 | Dose dependent antiproliferative effects of complex 50 in comparison with the standard drug 5-FU. | 193 |
| Figure 4.30 | Dose dependent antiproliferative effects of complex 51 in comparison with the standard drug 5-FU. | 193 |
| Figure 4.31 | Dose dependent antiproliferative effects of proligand 26 and complex- 52 in comparison with the standard drug 5-FU. | 194 |
| Figure 4.32 | Dose dependent antiproliferative effects of complex 53 in comparison with the standard drug 5-FU on the human colon cancer cell lines. | 196 |
| Figure 4.33 | Dose dependent antiproliferative effects of proligand 31 and its respective complex 57 in comparison with the standard drug 5-FU on the human colon cancer cell lines. | 196 |

| | | |
|-------------|--|-----|
| Figure 4.34 | Images of human colorectal cell lines showing the effects of proligand- 31 and complexes 53 & 57 . (cell images taken under a light microscope at $\times 200$ magnifications with a digital camera). | 197 |
| Figure 4.35 | Dose dependent antiproliferative effects of proligand 27 and the respective complex 53 in comparison with the standard drug Tamoxifen on the breast cancer cell lines. | 199 |
| Figure 4.36 | Dose dependent antiproliferative effects of proligand 28 and the respective complex 54 in comparison with the standard drug Tamoxifen on the breast cancer cell lines. | 199 |
| Figure 4.37 | Dose dependent antiproliferative effects of proligand 29 and the respective complex 55 in comparison with the standard drug Tamoxifen on the breast cancer cell lines. | 200 |
| Figure 4.38 | Dose dependent antiproliferative effects of proligand 30 and the respective complex 56 in comparison with the standard drug Tamoxifen on the breast cancer cell lines. | 200 |
| Figure 4.39 | Dose dependent antiproliferative effects of proligand 31 and the respective complex 57 in comparison with the standard drug Tamoxifen on the breast cancer cell lines. | 201 |
| Figure 4.40 | Dose dependent antiproliferative effects of complex 53 in comparison with the standard drug 5-FU against the human epitheloid cervix carcinoma (HeLa) cell lines. | 203 |
| Figure 4.41 | Dose dependent antiproliferative effects of complex 54 in comparison with the standard drug 5-FU against the human epitheloid cervix carcinoma (HeLa) cell lines. | 204 |
| Figure 4.42 | Dose dependent antiproliferative effects of complex 55 in comparison with the standard drug 5-FU against the human epitheloid cervix carcinoma (HeLa) cell lines. | 204 |
| Figure 4.43 | Dose dependent antiproliferative effects of complex 56 in comparison with the standard drug 5-FU against the human epitheloid cervix carcinoma (HeLa) cell lines. | 205 |
| Figure 4.44 | Dose dependent antiproliferative effects of proligand 31 and respective complex 57 in comparison with the standard drug 5-FU against the human epitheloid cervix carcinoma (HeLa) cell lines. | 205 |
| Figure 4.45 | Antimigration of the cancer cells data for proligand 31 after 6h and 12 h of administration of doses. | 207 |

| | | |
|-------------|---|-----|
| Figure 4.46 | Images of the breast cancer cell line (MCF-7) in the cell migration assay. The cells were grown in 6-well cell culture plates and a wound was created in the center of each well when the wells were confluent. These were then treated with proligand 31 in two concentrations: 6.25 and 12.5 $\mu\text{g}/\text{mL}$, and the images of the cells were taken under an inverted phase-contrast microscope at $\times 4$ magnification at 0 h (zero), 6 h and 12 h after the treatment with proligand 31 . | 208 |
| Figure 4.47 | Antimigration of the cancer cells data for complex 57 after 6h and 12 h of administration of doses. | 209 |
| Figure 4.48 | Images of the breast cancer cell line (MCF-7) in the cell migration assay. The cells were grown in 6-well cell culture plates and a wound was created in the center of each well after the wells were confluent. The cells were then treated with complex 57 in two concentrations 2.5 and 5 $\mu\text{g}/\text{mL}$ and the images of the cells were taken under an inverted phase-contrast microscope at $\times 4$ magnification at 0 h (zero), 6 h and after 12 h of treatment with the complex 57 . | 210 |
| Figure 4.49 | Percentages of cell survival after administration of different doses 6.25, 12.5 and 25 $\mu\text{g}/\text{ml}$ of proligand 31 on the breast cancer cell line. | 211 |
| Figure 4.50 | Photographs of the cell culture plates showing cell survival after administration of different doses 6.25-25 $\mu\text{g}/\text{mL}$ of proligand 31 on breast cancer cell line. | 212 |
| Figure 4.51 | Percentages of cell survival after administration of different doses 2.5, 5 and 10 $\mu\text{g}/\text{ml}$ of complex 57 on breast cancer cell line. | 213 |
| Figure 4.52 | Photographs of the cell culture plates showing the cell survival after administration of different doses 2.5-10 $\mu\text{g}/\text{mL}$ of complex 57 on breast cancer cell line. | 214 |
| Figure 4.53 | Comparison between the anticancer activities of mono, di, tri and tetra NHC proligands and their respective Ag(I) complexes against the human colon cancer cell lines. | 217 |
| Figure 4.54 | Data showing the overall mean percentage inhibition of proliferation of proligands and complexes of the mono, di, tri and tetra NHC compounds having 10 carbon chain substitutions against the human colon cancer cell lines. | 219 |
| Figure 4.55 | Plasma membrane structure and composition (adapted from onlinetutoring.edublogs.org). | 220 |

Figure 5.1 Structures of proposed NHC-Ag(I) complexes for future studies. 225

LIST OF SCHEMES

| | | Page |
|-------------|---|-------------|
| Scheme 1.1 | Synthesis of first Fischer carbene complex. | 3 |
| Scheme 1.2 | Synthesis of first Schrock carbene complex. | 3 |
| Scheme 1.3 | Attempted synthesis of free carbene by Wanzlick. | 6 |
| Scheme 1.4 | Synthesis of first stable free carbene by Arduengo. | 7 |
| Scheme 1.5 | Synthesis of first NHC transition metal complexes by (a) Wanzlick and (b) Öfele. | 11 |
| Scheme 1.6 | Synthesis of NHC alane adduct. | 13 |
| Scheme 1.7 | Ligand transfer reaction reaction from W(0) to Au(I). | 14 |
| Scheme 1.8 | Synthesis of NHC transition metal complex by the cleavage of electron rich enetetraamines. | 15 |
| Scheme 1.9 | Synthesis of first NHC-Ag(I) complex by Arduengo using free carbene. | 16 |
| Scheme 1.10 | General representation of <i>in situ</i> deprotonation methods for the synthesis of imidazolium/benzimidazolium derived NHC-Ag(I) complexes. | 17 |
| Scheme 1.11 | Some transmetallation reactions involving NHC-Ag(I) complexes (a) (Huang et al., 2014), (b) (Simons et al., 2003), (c) (Chianese et al., 2003). | 25 |
| Scheme 3.1 | Synthesis of <i>N, N</i> - <i>n</i> -alkylbenzimidazolium bromides (1-8). | 104 |
| Scheme 3.2 | Synthesis of tetramethylene bis(<i>N</i> - <i>n</i> -alkylbenzimidazolium bromide) (9-16). | 105 |
| Scheme 3.3 | Synthesis of 3-(2-bromoethyl)-1-substituted benzimidazolium bromides (17-21). | 106 |
| Scheme 3.4 | Synthesis of tris benzimidazolium bromides (22-26). | 107 |
| Scheme 3.5 | Synthesis of 1,2-bis(benzimidazol-1-ylmethyl)benzene. | 108 |

| | | |
|-------------|--|-----|
| Scheme 3.6 | Synthesis of tetrakis benzimidazolium bromides (27-31). | 109 |
| Scheme 3.7 | Synthesis of mono NHC-Ag(I) complexes (32-39). | 111 |
| Scheme 3.8 | Synthesis of di NHC-Ag(I) complexes (40-47). | 111 |
| Scheme 3.9 | Synthesis of tri NHC-Ag(I) complexes (48-52). | 112 |
| Scheme 3.10 | Synthesis of tetra NHC-Ag(I) complexes (53-57). | 113 |

LIST OF ABBREVIATIONS

| | |
|------------------|---|
| NHC | <i>N</i> -heterocyclic carbene |
| Ar | Arene |
| Mes | Mesityl |
| DMSO | Dimethyl sulfoxide |
| THF | Tetrahydrofuran |
| DCM | Dichloromethane |
| OAc | Acetate |
| ^t Bu | Tertiary butoxide |
| Cod | Cyclooctadiene |
| h/hr | Hour |
| RT | Room temperature |
| Anal. | Analysis |
| Calc. | Calculated |
| <i>J</i> | Coupling constant |
| Å | Angstrom |
| HIFBS | Heat inactivated foetal bovine serum |
| PBS | Phosphate buffer saline |
| PS | Penicillin/streptomycin |
| DMEM | Dulbecco's Modified Eagle Medium |
| MTT | Methylthiazolyldiphenyl-tetrazolium bromide |
| IC ₅₀ | Half maximal inhibitory concentration |
| RPMI | Roswell Park Memorial Institute |

ORTEP

Oak Ridge Thermal Ellipsoid Plot

NA

Not active

SINTESIS, PENCIRIAN DAN PENILAIAN POTENSI SITOTOKSIK *IN VITRO* KOMPLEKS ARGENTUM(I) MONO, DI, TRI DAN TETRA *N*-HETEROSIKLIK KARBENA

ABSTRAK

Tesis ini memaparkan tentang sintesis, pencirian dan penilaian potensi sitotoksik *in vitro* untuk dua puluh enam kompleks baru mono, di, tri dan tetra NHC-Ag(I) yang dihasilkan daripada dua puluh enam garam baru mono, bis, tris dan tetrakis benzimidazolium. Empat siri garam yang mempunyai terminal *N*-pergantian yang simetrikal telah disediakan. Lapan jenis garam baru bergantian mono benzimidazolium yang bersimetri (**1-8**) telah disintesis menggunakan *N-n*-alkilasyen ($n=3-10$) yang berperingkat, manakala lapan jenis garam baru bis benzimidazolium bergantian yang bersimetri *N*-alkil (**9-16**) telah dihasilkan daripada satu sistem tetrametilin yang bersilang. Sintesis untuk garam tris dan tetra benzimidazolium telah dijalankan menggunakan cadangan dan skema yang direka baru yang melibatkan generasi lima baru pelopor garam (**17-21**), antaranya 3-(2-bromoetil)-1-bergantian benzimidazolium bromida (benzil/ *n*-butil/ cyclopentil/ 2-methylenebenzoni-tril/ *n*-decil). Pelopor-pelopor ini telah bertindak balas dengan benzimidazol menghasilkan lima generasi baru garam benzimidazolium tris bersilang dimetilin (**22-26**). Tambahan lagi, lima garam benzimidazolium asiklik tetra baru telah didapati melalui tindak balas garam pelopor yang pada permulaannya adalah 1,2-bis(benzimidazol-1-ilmetil)benzena yang telah disintesis. Garam untuk keempat-empat siri telah ditukar kepada kompleks NHC-Ag(I) masing-masing menggunakan kaedah *in situ* deprotonasi dan pengkompleksan melibatkan Ag₂O,

menghasilkan pengasingan 26 kompleks baru NHC-Ag(I) (**32-57**). Struktur untuk semua garam dan kompleks NHC-Ag(I) telah dibuktikan menggunakan satu kombinasi spektra (FTIR, ^1H , ^{13}C -NMR) dan analisis (CHN) elemental. Kajian hablur sinaran-X untuk kompleks (**38**, **39**, **45**, **47** and **55**) telah menunjukkan motif pengikatan untuk kompleks mono, di dan tetra NHC-Ag(I). Potensi antikanser in vitro untuk kesemua empat siri garam dan kompleks NHC-Ag(I) masing-masing telah diperiksa terlebih dahulu melawan bahagian sel kanser kolon (HCT116) manusia. Terdapat peningkatan dalam aktiviti antikanser apabila peningkatan panjang rantai penggantian dalam kes siri mono dan di, yang mana siri di telah dijumpai lebih aktif berbanding siri mono. Siri tri dan tetra menunjukkan aktiviti yang dipilih terhadap bahagian sel kanser kolon manusia, dan kemudiannya telah diperiksa melawan bahagian sel kanser payudara (MCF-7) dan kanser serviks (HeLa), di mana kesemua kompleks telah menunjukkan aktiviti antikanser. Dalam semua siri, kompleks NHC-Ag(I) telah dijumpai lebih aktif daripada proligan masing-masing. Pengkajian tentang kesan penggantian terhadap potensi antikanser melawan bahagian kanser sel yang dipilih telah membuktikan bahawa garam dan kompleks yang mempunyai rantai *n*-alkil yang paling panjang (*n*-dekil) daripada setiap siri yang dikaji adalah paling aktif. Aktiviti ini mungkin disebabkan oleh peningkatan lipofilisiti untuk penggantian *n*-dekil. Dalam untuk mendapatkan lebih pencerahan tentang mekanisma tindakan kompleks-kompleks baru tetra NHC-Ag(I) yang direka dan garam masing, kompleks **57** and garam **31**-nya telah dipilih untuk pengkajian seterusnya dalam asas indeks pemilihan. Sebatian yang dipilih telah dikaji untuk mekanisma perencatan migrasi sel dan perencatan pembentukan koloni. Kompleks dan garamnya yang dipilih telah dijumpai untuk menunjukkan potensi antikanser dengan perencatan pembentukan koloni dan migrasi sel kanser.

**SYNTHESIS, CHARACTERIZATION AND *IN VITRO* EVALUATION OF
CYTOTOXIC POTENTIAL OF MONO, DI, TRI AND TETRA
N-HETEROCYCLIC CARBENE SILVER(I) COMPLEXES**

ABSTRACT

This thesis presents the synthesis, characterization and *in vitro* evaluation of cytotoxic potential of twenty six new mono-, di-, tri- and tetra-NHC-Ag(I) complexes derived from twenty six new mono-, bis-, tris- and tetrakis-benzimidazolium salts. The four series of salts with symmetrical terminal *N*-substitution were prepared. The eight new symmetrically substituted mono benzimidazolium salts (**1-8**) were prepared by stepwise *N-n*-alkylation (n=3-10), while the eight new symmetrically *n*-alkyl substituted bis benzimidazolium salts (**9-16**) were derived from tetramethylene linked system. The synthesis of tris and tetrakis benzimidazolium salts was carried out by newly designed schemes that involved the generation of the five new precursor salts (**17-21**), namely 3-(2-bromoethyl)-1-substituted benzimidazolium bromide (benzyl/ *n*-butyl/ cyclopentyl/ 2-methylenebenzotrile/ *n*-decyl). These precursors were reacted with benzimidazole thus resulting in the generation of five new dimethylene linked tris benzimidazolium salts (**22-26**). Another five new acyclic tetrakis benzimidazolium salts (**27-31**) were obtained by reacting the precursor salts (**17-21**) with the initially synthesized 1,2-bis(benzimidazol-1-ylmethyl)benzene. The salts of all the four series were converted to their respective NHC-Ag(I) complexes using the *in situ* deprotonation and complexation method involving Ag₂O, thus resulting in the formation of twenty six new NHC-Ag(I) complexes (**32-57**). The structures of all the

salts and NHC-Ag(I) complexes were established by a combination of spectral (FTIR, ^1H , ^{13}C -NMR) and elemental (CHN) analysis, while the X-ray crystal studies of complexes (**38**, **39**, **45**, **47** and **55**) revealed the bonding motifs of mono, di and tetra NHC-Ag(I) complexes. The *in vitro* cytotoxic potential of all the four series of salts and their respective NHC-Ag(I) complexes was preliminary tested against human colon cancer cell lines (HCT116). There was an increase in cytotoxic activities with increase in the alkyl chain length of substituents in the mono- and di-NHC series, while the di-NHC series was found to be more active as compared to the mono-NHC series. On the other hand tri- and tetra-NHC series showed selective activities on human colon cancer cell line and were further tested against breast cancer (MCF-7) and cervical cancer cell line (HeLa) of which all the complexes in both series displayed anticancer activities. In all the above mentioned series, the NHC-Ag(I) complexes were found to be more active than their respective proligands. The investigation of the effect of substitutions on cytotoxic potential on the selected cancer cell lines showed that the salts and complexes having the longest *n*-alkyl chain (*n*-decyl) in each series were the most potent. That may be attributed to the increased lipophilicity of the *n*-decyl substituent. In order to gain preliminary insights into the mode of cytotoxic activity of the newly designed tetra NHC-Ag(I) complexes and their respective salts, complex **57** and its respective salt **31**, were selected for investigation. The selected complex and its respective salt were found to display cytotoxic potential by inhibiting the colony formation and migration of cancer cells.

CHAPTER 1

INTRODUCTION

1.1 The Carbenes

Carbenes are uncharged species comprising a divalent carbon atom with six valence electrons. Depending on the geometry at the carbene carbon atom, they can either be sp^2 or sp hybridized. The carbene carbon atom with a linear geometry is sp hybridized with two energetically degenerated p orbitals whereas the sp^2 hybridized carbon atom having a σ and a $p\pi$ orbital adopts a bent geometry. The carbon atom in most carbenes is sp^2 hybridized state as it is energetically more stable as compared to those with sp hybridized carbon (Hahn & Jahnke 2008).

The sp^2 hybridized carbenes can be further distinguished as either singlet or triplet carbenes depending on the multiplicity of the ground state which is determined by the relative energies of the σ and $p\pi$ orbitals. If the energy difference between the two orbitals is large, then the two nonbonding electrons will occupy the σ orbital with an antiparallel spin orientation leading to the singlet ground state. Conversely, if there is less energy difference, the nonbonding electrons will occupy the independent σ and $p\pi$ orbitals with a parallel spin orientation resulting in a triplet ground state (Figure 1.1). The ground state multiplicity of carbenes determines their properties and reactivity (Schuster, 1987).

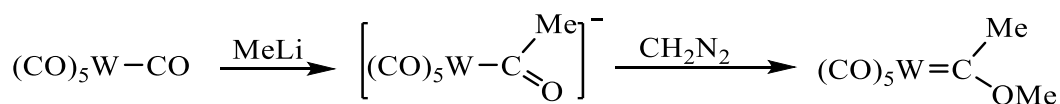


Figure 1.1: Representation of spin multiplicities of sp^2 hybridized carbenes.

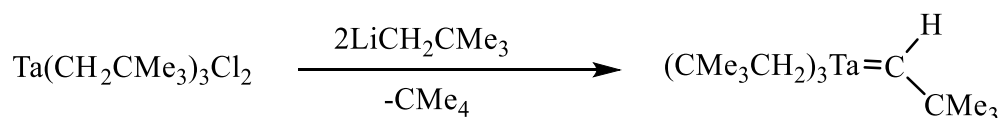
It is generally thought that the substituents at the carbene carbon atom control the multiplicity of the ground state owing to their steric and electronic effects. In case of inductive effect, σ - electron withdrawing substituents favour the singlet ground state as they lower the energy of the nonbonding σ orbital through their negative inductive effect. Alternatively, σ -electron donating substituents favour the triplet ground state by decreasing the energy gap between the σ and $p\pi$ orbitals. In addition to the inductive effects, the mesomeric effect of the substituent also plays a vital role in determining the multiplicity of the carbene. The π -electron donating substituents raises only the energy of the $p\pi$ orbital, increasing the energy gap of σ and $p\pi$ orbitals which also results in a stable singlet ground state. On the other hand, the π -electron accepting substituents lend the carbene in a singlet ground state with almost linear geometry (Schoeller, 1980).

The efforts for the synthesis and isolation of free carbenes started as early as 1835 by J. B. Dumas who attempted to dehydrate methanol to get methylene. The first firm structural evidence for the formation of dichloro carbene was reported by Doering (von E. Doering & Hoffmann, 1954) as an intermediate in cyclopropanation reaction. At that time, carbenes were considered as highly reactive, short lived intermediates in organic transformations. Soon after that, the concept of double bond between transition metals and carbon was introduced by Fischer with the first

recognized heteroatom stabilized carbene complex in organometallic chemistry (Scheme 1.1) (Fischer & Maasbol, 1964). Afterwards, a number of tantalum carbene complexes were reported by Schrock (Scheme 1.2) (Schrock, 1974). Around the same time Wanzlick introduced the concept of *N*-heterocyclic carbenes and later in 1968, metal complexes with *N*-heterocyclic carbene ligands were reported. After the discovery of these metal carbene complexes, the exploration of their chemistry began.



Scheme 1.1: Synthesis of the first Fischer carbene complex.



Scheme 1.2: Synthesis of the first Schrock carbene complex.

1.2 Classification of carbenes

During the development of metal-carbene complexes, three different patterns of reactivity and bonding emerged resulting in their classification into different types as described below.

1.2.1 Fischer carbenes

Fischer carbenes are singlet carbenes with two nonbonding electrons in the σ orbital having a vacant $p\pi$ orbital and at least one good π -donor substituent. The

metal-carbene chemical bond is formed by the donation of the lone pair from the σ orbital of the carbene to an empty d_σ orbital of that metal. The empty $p\pi$ orbital of carbene is stabilized by π -donation from the substituent as well as π -back-bonding from the filled d_π orbital of the metal. As the late transition metals (low oxidation state) have stabilized d_π orbitals and are good π -donors, they tend to stabilize the Fischer type carbenes. This bonding pattern leaves the carbon electrophilic because the direct carbene to metal donation is only partly compensated by metal to carbene π -back-donation (Figure 1.2).

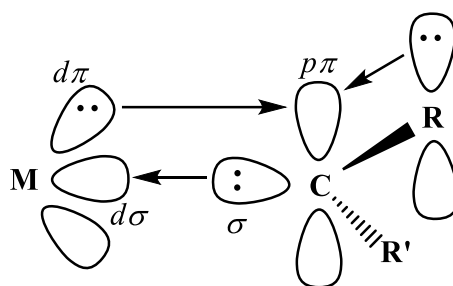


Figure 1.2: Carbene to metal bonding in Fischer carbene.

1.2.2 Schrock carbenes

Schrock carbenes are triplet carbenes with both σ and $p\pi$ orbitals singly occupied. These carbenes must have substituents that are not π -donors, such as alkyl groups, in order to inhibit the repulsions of electrons. In this case, the carbene forms two covalent bonds with the metal each polarized towards the carbon making it nucleophilic (Figure 1.3). Schrock carbenes form complexes with early transition metals (high oxidation state).

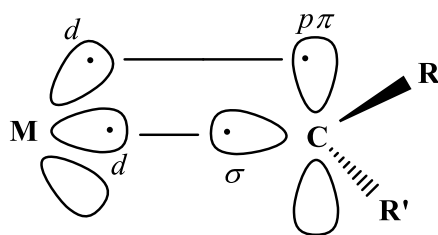


Figure 1.3: Carbene to metal bonding in Schrock carbene.

1.2.3 *N*-heterocyclic carbenes

N-heterocyclic carbenes (NHCs) are singlet carbenes and have two adjacent π -donating nitrogen atoms. The NHCs bond to metals through the σ -donation of the carbene lone pair. The empty $p\pi$ orbital of the carbene is strongly stabilized by π -donation from the nitrogen atoms (Figure 1.4). This electron donation gives nucleophilic character to the NHCs and makes them excellent σ -donors to transition metals both in low and high oxidation states as well as to main group metals. Contrary to the Fischer and Schrock carbenes, the NHCs are stable, capable of independent existence and can be readily prepared.

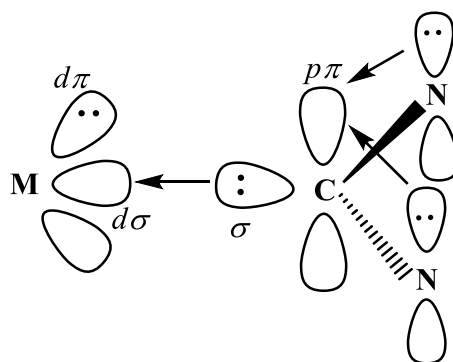
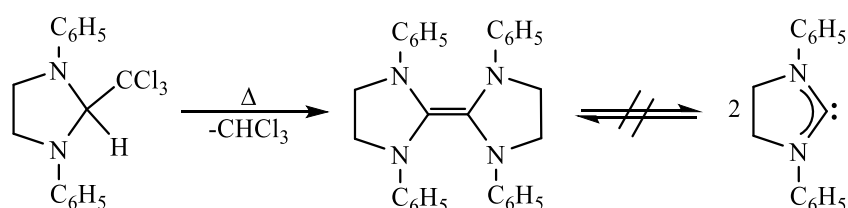


Figure 1.4: Carbene to metal bonding in *N*-heterocyclic carbene.

1.3 Emergence of *N*-heterocyclic carbenes

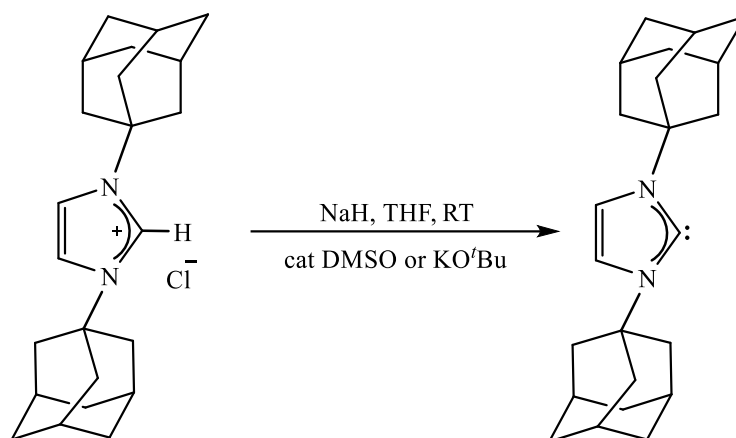
H.W. Wanzlick was the pioneer bringing NHC into focus in 1960. He hypothesized that the carbenes could be stabilized by the presence of amino substituents in *N*-heterocyclic systems based on the fact that the delocalization of six π -electrons in such systems would stabilize the carbene. He therefore tried to prepare and isolate 1,3-diphenylimidazolidin-2-ylidene by thermal elimination of chloroform, instead of NHC, only its dimer, the enetetraamine was obtained and consequently the postulated equilibrium between the monomer and the dimer could not be proven. (Scheme 1.3) (Wanzlick, 1962; Wanzlick & Kleiner, 1961; Wanzlick & Schikora, 1960). Furthermore, he attempted to prepare free NHC by the deprotonation of tetraphenylimidazolium perchlorate with potassium *tert*-butoxide, although the expected free NHC could not be isolated, yet its intermediate formation was demonstrated (Schonherr & Wanzlick, 1970).



Scheme 1.3: Attempted synthesis of free carbene by Wanzlick.

In 1991, Arduengo and co-workers reported the successful synthesis and isolation of the first crystalline free carbene that was stable in the absence of oxygen and moisture. The stable 1,3-di-adamantyl-imidazol-2-ylidene was obtained by the deprotonation of 1,3-di-adamantyl-imidazolium chloride using one equivalent of

sodium hydride with a catalytic amount of DMSO anion or potassium tertiary butoxide in THF at room temperature (Arduengo III et al., 1991) (Scheme 1.4).



Scheme 1.4: Synthesis of the first stable free carbene by Arduengo.

The resulting carbene was found to be thermally stable with a melting point of 240-241°C without decomposition and it was also fully characterized and elucidated crystallographically. The isolation of this stable carbene initially led to the assumption that its stability is due to the steric bulk around it but further work by Arduengo negated this view where he successfully isolated a carbene with only methyl substituents on the heterocycle (Figure 1.5(a)) along with three more stable NHCs having different substitution patterns (Arduengo III, Dias, Harlow, et al., 1992) [Figure 1.5(b, c, d)]. The aromaticity of the NHC system which was initially considered as one of the necessary factors for the stability of free NHC was proven not to be of prime importance by the synthesis of stable imidazolin-2-ylidene (Figure 1.5(e)) with non aromatic heterocycle (Arduengo III et al., 1995). All these NHCs were synthesized under the same experimental conditions. Later on, Arduengo and

co-workers were also successful in synthesizing free 1,3,4,5-tetraphenylimidazol-2-ylidene (Figure 1.5(f)) by the modification of Wanzlick's experimental procedure.

The avenue opened up by Arduengo to the isolation of free carbene had led others to synthesize and isolate stable carbenes by applying different methods. Kuhn and co-worker reported the synthesis of alkyl substituted imidazol-2-ylidene by the reduction of imidazole-2-(3H)-thione using potassium in boiling THF (Kuhn & Kratz, 1993). The first commercially available carbene derived from a triazole (1,2,4-triazol-5-ylidene) was synthesized by Enders and co-workers (Enders et al., 1995). Herrmann and co-workers reported a number of functionalized imidazoline-2-ylidenes by introducing a new synthetic strategy involving the use of liquid ammonia in aprotic organic solvent along with a base (Herrmann et al., 1996). This new method of carbene generation offers advantage over other reported methods in terms of reaction time as carbenes can be generated in few minutes and in high yield. The use of liquid ammonia serves to increase the solubility of imidazolium salts in organic solvents and also increases the acidity of C-2 protons through hydrogen bonding. Danopoulos and co-workers reported the 2,6-bis(arylimidazol-2-ylidene)pyridine which was the first stable pincer based bis carbene (Danopoulos et al., 2002).

In addition to the cyclic amino carbenes, Alders and co-workers had successfully generated an acyclic amino carbene, bis(diisopropylamino)carbene thus showing that the amino substituent plays a vital role in the stabilization of carbenes without the need of a cyclic structure (Alder et al., 1996). In the studies focussing on NHC, apart from the five membered *N*-heterocyclic carbenes, a stable six-membered NHC, 1,3-diisopropyl-3,4,5,6-tetrahydropyrimid-2-ylidene was also reported (Alder

et al., 1999). The carbenes of the class imidazol-2-ylidene still form the major type of stable NHCs.

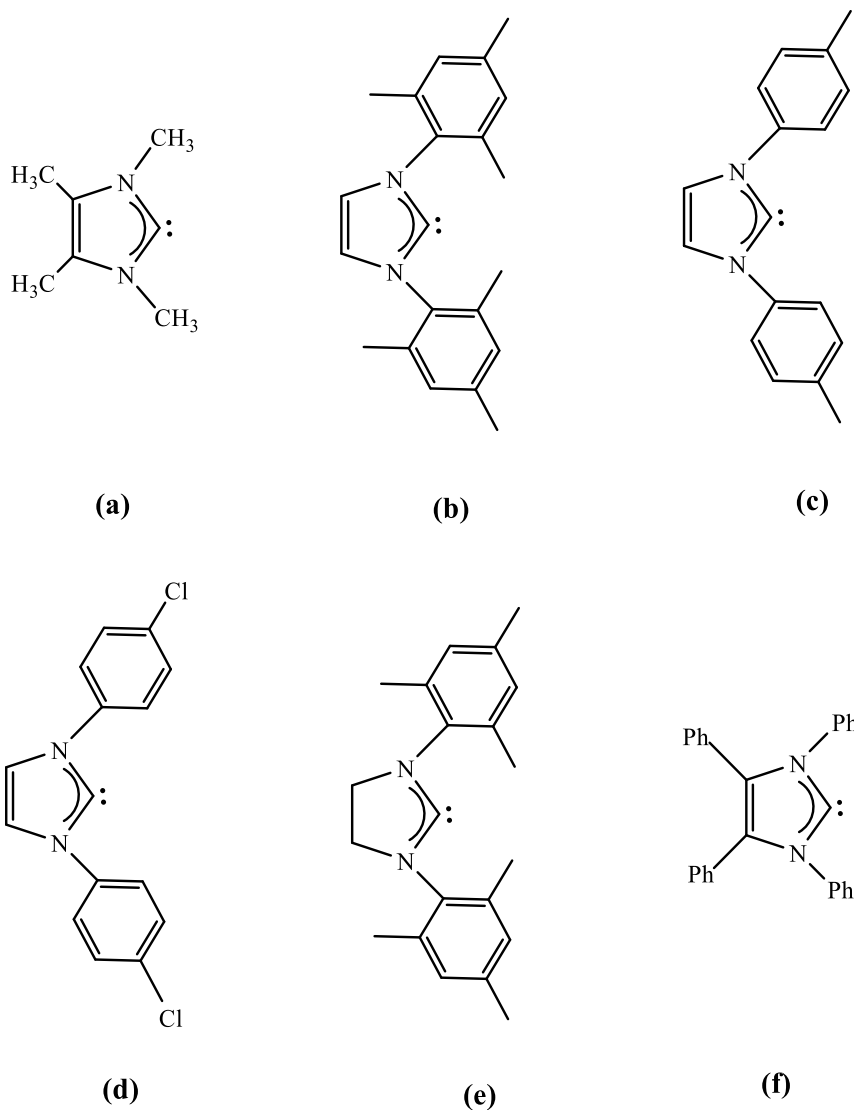


Figure 1.5: Structures of reported stable carbenes (a-f) by Arduengo.

From the above discussed literature, one can conclude that *N*-heterocyclic carbenes can be of different classes depending on the *N*-heterocyclic system, from which they are generated and therefore named accordingly. The systematical names of the parent heterocyclic compounds are given a suffix that is determined by the

kind of heterocyclic system, followed by the addendum –ylidene. The term “ylidene” refers to a compound in which two hydrogens are replaced by a pair of electrons hereby referring to the carbene and is mentioned along with the position of the carbene carbon in the *N*-heterocyclic system. Figure 1.6 depicts some of the most common classes of *N*-heterocyclic carbenes.

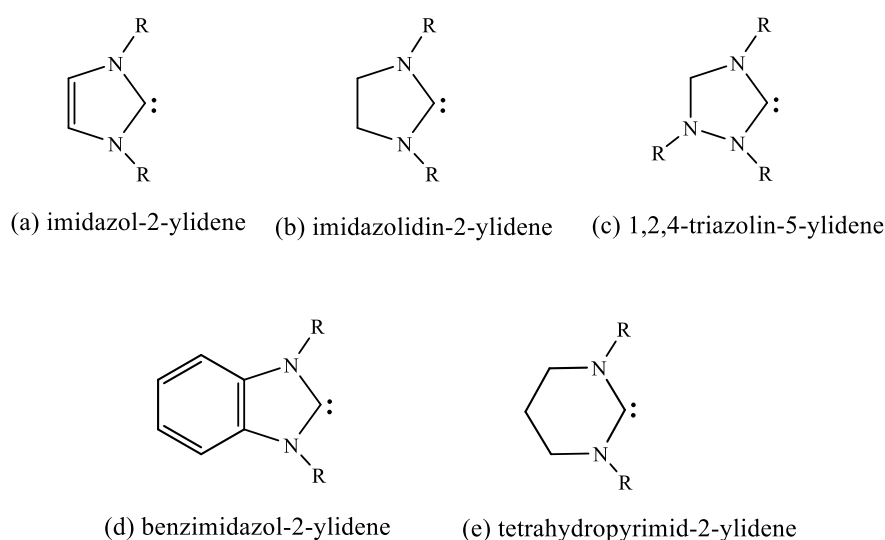


Figure 1.6: Structures of some of the most commonly applied classes of NHCs.

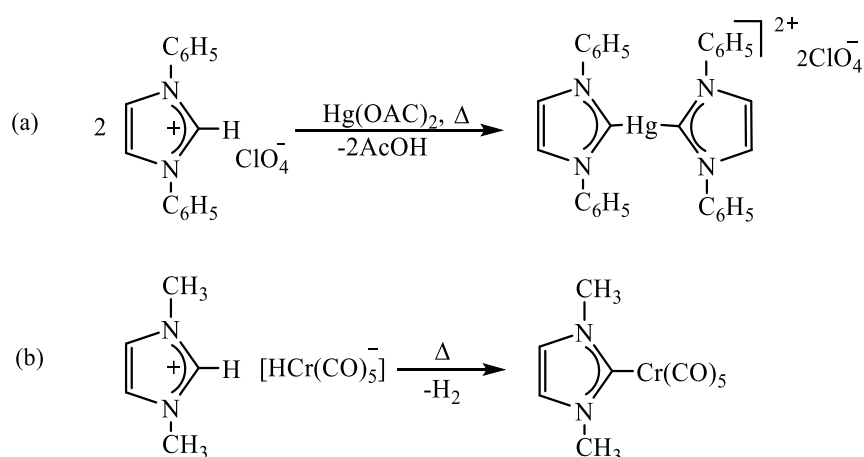
1.3.1 *N*-heterocyclic carbene complexes

NHCs as strong nucleophiles and excellent σ -donors, form adducts with virtually all the elements of the periodic table. The NHC complexes with transition metals were brought into focus even before the synthesis and isolation of the first reported free *N*-heterocyclic carbene, while with main group elements, the complexes began to be explored soon after the discovery of free NHC.

The most commonly used methods for the synthesis of NHC complexes are as follows:

1.3.1(a) *In situ* deprotonation of azolium salts

This method is based on the *in situ* deprotonation of the carbene precursor (azolium salt) which is achieved either by the use of metal source of sufficient basicity to deprotonate the azolium salts such as metal hydrides, alkoxides and acetates or by the addition of external bases such as potassium *tert*-butoxide, sodium hydride, sodium hydroxide, triethylamine to the metal source (Weskamp et al., 2000). The *in situ* deprotonation is the first known synthetic route for the formation of NHC transition metal complexes as demonstrated independently by Wanzlick and Öfele (Öfele, 1968; Wanzlick & Schonherr, 1968) [Scheme 1.5 (a,b)]. This method has also been reported for the synthesis of NHC complexes with rare earth metals (Clark et al., 2014; Gu et al., 2015; Lv & Cui, 2008; Wang et al., 2006). Most of the literature related to NHC transition metal complexes focuses on this method as it offers the advantage that the free carbene does not have to be isolated.



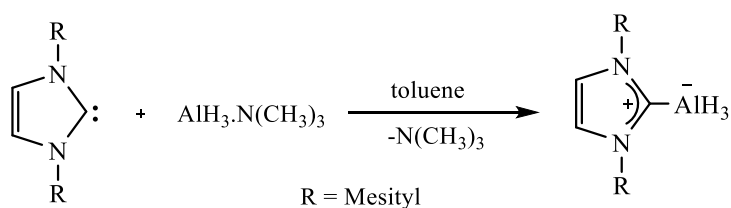
Scheme 1.5: Synthesis of the first NHC transition metal complexes by (a) Wanzlick and (b) Öfele.

1.3.1(b) Free carbene route

In this method, first the free NHC is generated by the deprotonation of azolium salts using strong bases such as KH, NaH or KO^tBu and the subsequent reaction of the free carbene with appropriate metal/element source yields the NHC complex. This is a useful method for those azolium salts that could generate free NHCs. Arduengo and coworkers, soon after the isolation of the first free stable NHC, reported the synthesis of a variety NHC transition metal complexes of Ag, Cu, Ni, Pt and Zn by such method (Arduengo et al., 1993; Arduengo et al., 1994) and it is still in use for the synthesis of different transition metal complexes (Alcarazo, 2005; Tapu, 2016). The rare earth metals have also been reported to form stable adducts with NHCs in high yields by utilizing this method (Herrmann et al., 1994); (Arduengo et al., 1994; Ferrence et al., 2006; Herrmann et al., 1997; Mehdoui et al., 2005; Schumann et al., 2007; Schumann et al., 1994a, 1994b).

The free carbene route is most commonly used for the synthesis of NHC complexes with main group metals and elements. The derivatives of alkali and alkaline earth metals have been reported to form stable monomeric as well as dimeric adducts with NHCs (Alder et al., 1999; Arduengo et al., 1998; Maddock et al., 2015). NHCs strongly coordinate to a multitude of different *p*-block species, leading to adducts with a variety of different structures. For example, among group 13 the first NHC-alane adduct, imidazol-2-ylidene-AlH₃ was reported by Arduengo (Arduengo et al., 1992) (Scheme 1.6). Imidazol-2-ylidenes form stable monomeric adducts with B, Al, Ga derivatives which have been isolated as trihydrides, trimethyl and trichlorides (Abernethy et al., 2000; Kuhn et al., 1993; Marion et al., 2007). From the group 14 species, 1,3-mesityl-imidazolin-2-ylidenes, when reacted with methyl

iodide, form stable olefin along with the formation of imidazolium salt (Arduengo, Davidson, et al., 1997). The imidazol-2-ylidenes can form stable tetravalent, pentavalent and hexavalent adducts with silicon and tin derivatives (Filippou et al., 2013; Jones et al.; Kuhn et al., 1995). The cyclic oligomers of phosphorous and arsenic among group 15 species form stable adducts with 1,3-dimesitylimidazol-2-ylidene (Arduengo, Calabrese, et al., 1997). The chalcogens (O, S, Se, Te) with imidazol-2-ylidenes have been reported to give stable imidazolium chalcogenides (Enders et al., 1995; Huffer et al., 2013). Among halogens, stable adducts with iodine and chlorine have been obtained by the reaction of imidazol-2-ylidenes with iodine and dichloroethane, respectively (Kuhn et al., 1998; Kuhn et al., 1993).

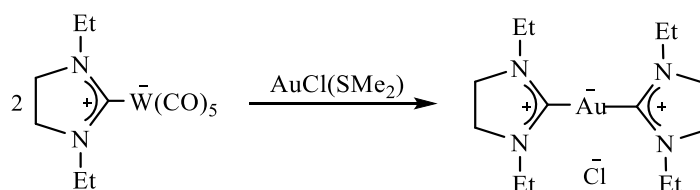


Scheme 1.6: Synthesis of NHC alane adduct.

1.3.1(c) Ligand transfer reactions

It involves the transfer of NHC ligand from one labile metal to another. Liu and co-workers have reported the successful transfer of NHC ligand from the NHC complexes of W(0), Cr(0), Mo(0) to Pd(II), Pt(II), Rh(I) and Au(I) (Liu, 1998) (Scheme 1.7). The use of NHC-Ag(I) complexes as NHC transfer agents was introduced by Wang and Lin and is found promising in getting a variety of other transition metal complexes (Wang & Lin, 1998). Transmetalation involving the use of NHC-Ag(I) is discussed in detail under applications of NHC-Ag(I) complexes.

Apart from NHC-Ag(I), the use of NHC-Hg(II) complexes as NHC-transfer agents have also been reported to give successful transmetallation results (Baker et al., 2009; Lin & Vasam, 2007; Meyer et al., 2012). The NHC-Cu(I) complexes have also been reported to readily transfer the NHC ligand to Pd(II) and Au(I) (Furst, 2010) as well as Rh(I) and Ir(I) (Bidal, 2016). Apart from transition metal complexes, NHC-Li complexes have also been reported as effective carbene transfer agents (Arnold et al., 2003; Arnold et al., 2004; Liddle & Arnold, 2005). A variety of transition metal complexes such as Au(I), Cu(I), Cu(II), Ni(II), Pd(II), Pt(II), Rh(I), Rh(III), Ir(I), Ir(III), Ru(II), Ru(III) and Ru(IV) can be obtained by this method.

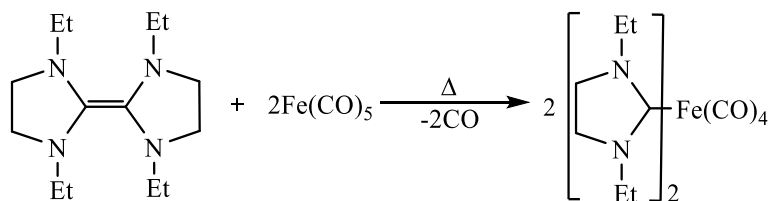


Scheme 1.7: Ligand transfer reaction from W(0) to Au(I).

1.3.1(d) Cleavage of enetetraamines

This method was introduced by Lappert and coworkers (Cardin, 1971). It involves the cleavage of electron rich enetetraamines (tetraaminoethylenes) into carbene monomers in the presence of coordinatively unsaturated electrophilic metal sources, resulting in the coordination of carbene with the metal center. This method has been successfully used for the synthesis of mono, bis, tris and tetrakis carbene complexes of various metals such as Cr, Mo, W, Mn, Fe, Ru, Os, Co, Rh, Ir, Ni, Pd, Pt, Au, Hg and Sn in different oxidation states (Cetinkaya et al., 1994; Hahn et al.,

2001; Hitchcock et al., 1978; Karaca et al., 2015; Lappert, 2005; Lappert & Pye, 1977) (Scheme 1.8).



Scheme 1.8: Synthesis of NHC transition metal complex by the cleavage of electron rich enetetraamines.

1.4 *N*-heterocyclic carbene silver(I) complexes

Among the NHC-transition metal complexes, NHC-Ag(I) complexes have gained much focus due to their simpler synthetic strategies and stability, diverse structural architectures and various promising applications. All these aspects of NHC-Ag(I) complexes are discussed below.

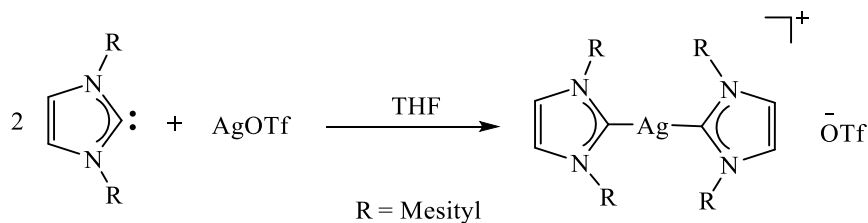
1.4.1 Synthesis of *N*-heterocyclic carbene silver(I) complexes

NHC-Ag(I) complexes can be successfully synthesized by the following two methods:

1.4.1(a) The free carbene method

The first NHC-Ag(I) complex reported by Arduengo was obtained by the direct reaction of a preformed 1,3-dimesitylimidazol-2-ylidene with silver triflate, thus resulting in the formation of a bis(carbene) Ag(I) adduct (Arduengo et al., 1993) (Scheme 1.9). NHC-Ag(I) complexes derived from five, six and seven membered free NHCs have also been reported (Iglesias, 2008). As this method

requires the initial generation of free carbene, it is limited to those azolium salts that can generate stable carbenes.



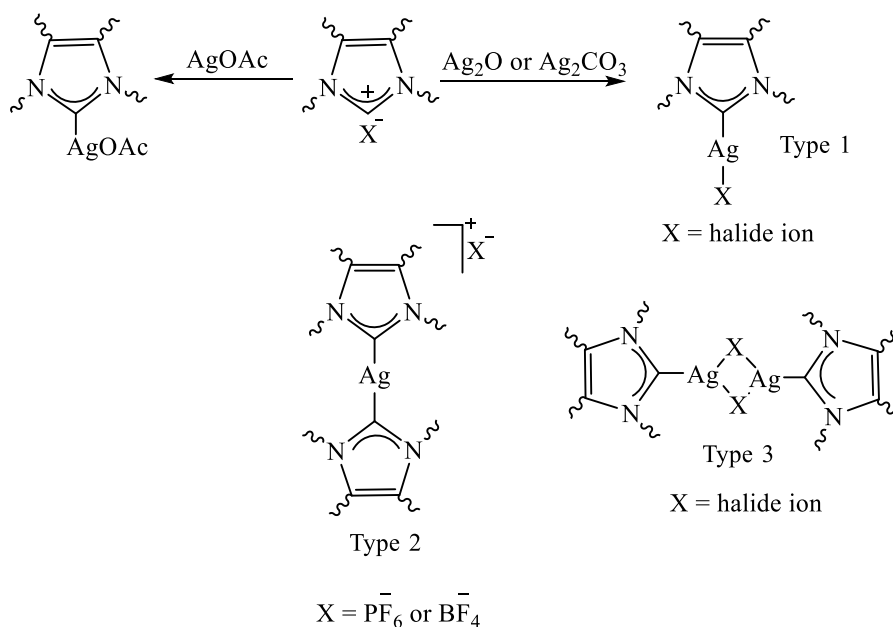
Scheme 1.9: Synthesis of the first NHC-Ag(I) complex by Arduengo using free carbene.

1.4.1(b) The *in situ* deprotonation method

The *in situ* deprotonation of azolium salt and complexation of resulting carbene with Ag(I) can be accomplished either by the use of a silver base, Ag₂O or the basic silver salts like AgOAc and Ag₂CO₃ (Scheme 1.10).

The first introduced *in situ* deprotonation method involved the use of silver acetate as a silver base to deprotonate 1,2,4-trisubstituted triazolium salt, resulting in the formation of a polymeric NHC-Ag(I) complex (Guerret et al., 1997). This method has now been used for the preparation of NHC-Ag(I) acetate complexes (Hindi et al., 2008; Patil et al., 2011). In 1998, Wang and Lin introduced a new method which involved the use of silver oxide (Wang & Lin, 1998). This method has gained much popularity and is most commonly used for the preparation of NHC-Ag(I) complexes. It involves the reaction of azolium salt with Ag₂O, resulting in deprotonation of C2 carbon (precarbenic carbon) and complexation of the resulting carbene with Ag(I) at the same time. This reaction requires no external base and special reaction conditions like inert atmosphere and for the most part, it is carried

out at room temperature with the exception of azolium salts with steric bulk around C2 carbon that needs refluxing (Tulloch et al., 2000). For this method, a number of different solvents like dichloromethane, dichloroethane, acetone, methanol, acetonitrile, DMSO, DMF, water and solvent mixtures can also be used. The resulting NHC-Ag(I) complexes are stable, high in yield and have an added advantage of being excellent carbene transfer agents to obtain other transition metal complexes (Lin & Vasam, 2007; Lu et al., 2012).



Scheme 1.10: A general representation of *in situ* deprotonation methods for the synthesis of imidazolium/benzimidazolium derived NHC-Ag(I) complexes.

Another method of *in situ* deprotonation and complexation which involves the use of silver carbonate was reported in 2000 (Tulloch et al., 2000). This method offers longer reaction times and is of limited use, therefore the Ag₂O route remains the preferred one. Most of the literature known NHC-Ag(I) complexes have been reported to be synthesized utilizing Ag₂O (Haque et al., 2013; Karataş et al., 2016; Samanta et al., 2015; Segarra et al., 2014)

1.4.2 Classification of *N*-heterocyclic carbene silver(I) complexes

The NHC metal complexes can be classified taking into account either the number of NHC unit per ligand molecule or by considering the number of metal centers per complex. However, the review articles dealing with the structural diversity of NHC metal complexes classify them mostly on the basis of NHC units per ligand (Garrison & Youngs, 2005; Poyatos et al., 2009). The NHC metal complexes are broadly classified into two main categories namely the mono-NHC and the poly-NHC, the latter can further be subdivided into different types.

The present classification is based on the number of carbene centres per ligand, of which the NHC-Ag(I) complexes can be of the following types;

1.4.2(a) Mono NHC-Ag(I) complexes

The mono-NHC (monodentate) ligands have one NHC unit per ligand molecule in the complex. Different bonding motifs of mono NHC-Ag(I) complexes can be obtained depending on whether the anion is noncoordinating or coordinating.

The mono NHC-Ag(I) complexes with noncoordinating anions exist as dimeric complexes with one Ag(I) ion bridging two NHC ligands giving rise to monometal diligand arrangement (Asekunowo & Haque, 2014) [Figure 1.7(a)]. Whereas with the coordinating anion, mainly halides, different structural variations are possible. The monomeric complexes with one Ag(I) ion coordinating to a carbene and an anion (Ramnial et al., 2003) [Figure 1.7(b)]; the mono NHC-Ag(I) complexes with bridging halides (Tulloch et al., 2000) [Figure 1.7(c)]; and the complexes forming staircases (Chen & Liu, 2003) (Figure 1.7(d)).

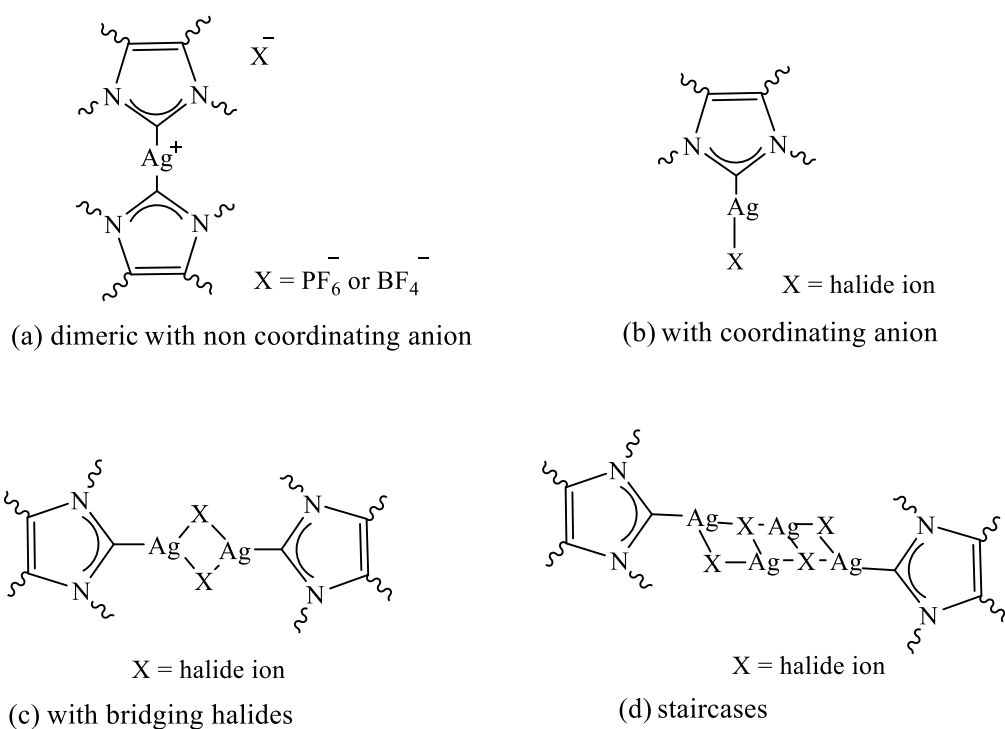


Figure 1.7: Structural variations of mono NHC-Ag(I) complexes.

1.4.2(b) Di NHC-Ag(I) complexes

The di-NHC (bidentate) ligands have a pair of NHC moieties connected via a bridging linker such as phenylene (Alcalde et al., 2007) (Haque et al., 2013), lutidinyl (Brown et al., 2009) (Haque et al., 2014), ether chain (Liu et al., 2007; Nielsen et al., 2003) or alkyl chain (Gil-Rubio et al., 2013) (Haque et al., 2013).

Depending on the flexibility and the size of the bridging linker, NHC-Ag(I) complexes can have four structural variations: the monometal monoligand complex [Figure 1.8(a)]; the bidentate monoligand and dimetal complexes [Figure 1.8(b)]; the dimetal diligand complex [Figure 1.8(c)] and the di-NHC-Ag(I) complexes derived from imidazolium linked cyclophanes (Baker et al., 2004) [Figure 1.8(d)].